LOCALIZED FEATURES OF CHAOTIC SYSTEM AND ATMOSPHERIC PREDICTABILITY

Li Zhijin (李志锦) and *Ji Liren* (纪立人)

Institute of Atmospheric Physics, Chinese Academy of Sciences, Beijing 100080

Received March 23, 1995

ABSTRACT

The localized features on chaotic attractor in phase space and predictability are investigated in the present study. It will be suggested that the localized features in phase space have to be considered in determining the predictability. The notions of the local instability including the finite-time and local-time instabilities which determine the growth rate of error are introduced, and the calculation methods are discussed in detail. The results from the calculation of the 3-component Lorenz model show that such instability, correspondingly the growth rate of error, varies dramatically as the trajectories evolve on the chaotic attractor. The region in which the growth rate of error is small is localized considerably, and is separable from the region in which the growth rate is large. The local predictability is of important interest. It is also suggested that such localized features may be the main cause for a great deal of case-to-case variability of the predictive skill in the operational forecasts.

Key words: chaotic attractor, localized feature, finite-time instability, local-time instability, predictability

I. INTRODUCTION

The atmospheric motion is characterized by its chaos (Lorenz 1963; 1984), and the evolution of atmospheric flow is essentially sensitive to its initial state. The small error in the initial atmospheric state will continually grow. Thus, there is an upper limit to the prediction of atmospheric behavior. Quite a few of studies have been contributed to determining such an upper limit. There were two kinds of studies. First, the upper limit to prediction of the model atmosphere is studied (e. g. Charney et al. 1966; Leith 1965; Smagorinsky 1963), which is convenient for the determination of the growth rate of error with different structures; second, the upper limit to prediction of the real atmosphere is determined. Lorenz (1969) pioneered the second kind of study. He attempted to find some atmospheric states in the historical data available which would be so close to each other that the differences between them were consistent with the practical observational error, and then make an estimation of the growth rate of the difference and the predictability. Though no such states were found, he still made an estimation based on simple extrapolation. Recently, the single long-time series was used to determine the atmospheric predictability (e. g. Wolf et al. 1985; Fraedrich 1987), in which the dynamical system is reconstructed with an embedding technique and some parameters, such as Lyapunov exponent and Reny entropy, are calculated. In spite of the difference in the methodology, thus in the estimate of the upper limit to prediction, the predictability of about

two weeks is commonly accepted. If the work from the development of concepts of predictability to the determination of deterministic predictability is referred to as the study of classic predictability, such study seems to come to the end.

Operational numerical weather prediction (NWP) has shown that there is a great deal of case-to-case variability of the predictive skill (Branstator 1986; Hollingworth et al. 1987). Whether does such variability only depend on the internal dynamics of the atmosphere itself or result from the deficiency of the NWP model? The theory of the classic predictability has not given the answer. Actually, it can not give the answer. It appears that the answer is related to the localized features of chaotic system (Lacarra et al. 1988; Mukougawa et al. 1991; Molteni et al. 1993). A few studies have discussed the growth of finite-time error for chaotic system. They showed that error growth may be much larger than that estimated from Lyapunov exponent and Reny entropy. We (Li and Ji 1994) have dynamically analyzed the cause of error growth, and indicated that the error growth rate varied considerably with the evolution of system states. It is thus of important interest to study the relationship between the variability of predictive skill and the localized features of chaotic system.

In the present study, finite-time and local-time instabilities will be introduced to describe the localized features of the chaotic system, and the corresponding calculation method will be discussed in detail. The famous Lorenz' s system will be used to exhibit the strong localized features of chaotic system.

II. LOCALIZED CHAOS IN PHASE SPACE

Before discussion of localized features of chaotic attractor itself, the attention is paid to whether chaotic attractors can coexist with periodic state or equilibrium state attractors. It seems to be difficult to answer theoretically such a question. Here the numerical method will be used to present a positive example.

Lorenz' s system has been extensively studied (for example, see review by Chou 1990). As is well-known, the equations of Lorenz' s system are

$$\frac{dx}{dt} = \sigma y - \sigma x, \tag{1}$$

$$\frac{dy}{dt} = \gamma x - y - xz, \tag{2}$$

$$\frac{dz}{dt} = -bz + xy. \tag{3}$$

In the present study, $\sigma = 10$ and $b = 8/3$. γ is served as a bifurcation parameter. If $\gamma \leqslant 1.0$, the system has a fixed point $(0, 0, 0)$, which is stable and called equilibrium state attractor. If $\gamma > 1.0$, there exist three fixed points: $(0, 0, 0)$, $(\pm \sqrt{b(\gamma-1)}, \pm \sqrt{b(\gamma-1)}, \gamma-1)$, and the fixed point $(0, 0, 0)$ becomes unstable. For $1 < \gamma \leqslant 24.74$, other two fixed points are stable. For $\gamma > 24.74$, all three fixed points become unstable, so no equilibrium state attractors will exist. For the last case, it has been shown (Chou 1990) that the system goes into chaos, i. e., the system possesses a chaotic attractor or a strange attractor.

We are now interested in the possibility of existence of chaos outside the basin of equilibrium state attractors. Such a phenomenon seems to be possible, but no theoretical

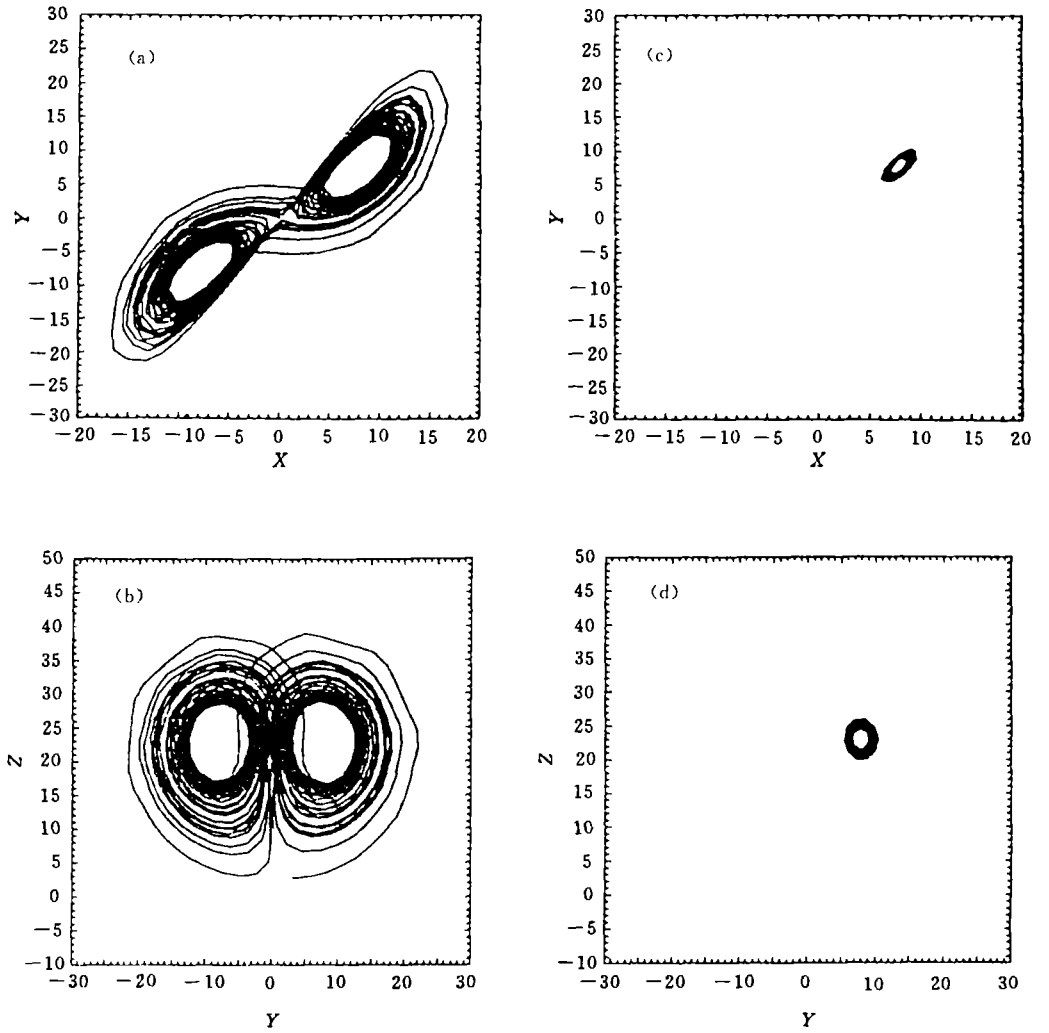

Fig. 1. Phase space evolution of Lorenz' s system with $\gamma=24.0$. (a) The trajectory in the X-Y plane starting from the initial state (1.0, 2.0, 3.0); (b) same as in (a), but for the Y-Z plane; (c) and (d) same as in (a) and (b) respectively, but for initial state (7.0, 7.0, 23.0).

evidence has been given and no positive example is presented. However, we will show a positive example. For $\gamma=24.0$, the system has two stable equilibrium states: (± 15.17, ± 15.17, 23.0). Trajectories will be shown in a 2D cut (Fig. 1). The trajectory starting from the initial state (1.0, 2.0, 3.0) is given in the X-Y plane in Fig. 1a and in the Y-Z plane in Fig. 1b. It can be seen that the evolution exhibits chaos. In fact, such evolution is evidently in a similar way to the standard Lorenz attractor, i. e. the chaotic attractor with $\gamma=28.0$. On the other hand, if a trajectory starts from the initial state lying in the neighborhood of the equilibrium state attractors, it will then gradually get into the attractors. Figures 1c and 1d present such a trajectory from the initial state (7.0, 7.0, 23.0).

The system has been integrated for a long time of 200 time units (corresponding to 10 000

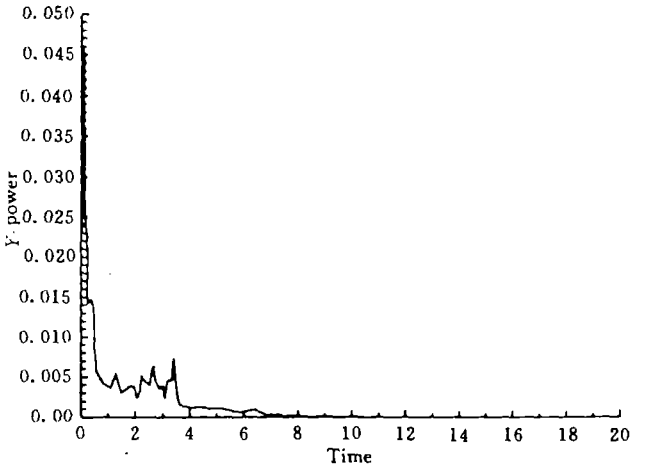

Fig. 2. The power spectrum of Y-component for integration time of 200 time units.

integration steps) to further verify the chaotic evolution for the initial state (1.0, 2.0, 3.0). Figure 2 shows the power spectrum. The spectral distribution is very broad, which is clearly indicative of the chaotic property of the system. We have also integrated the system with different time step sizes and calculation schemes, and obtained consistent results, which indicates that the chaos is independent of the used calculation method.

The coexistence of chaos and stable equilibrium states in phase space implies that the stability of equilibrium states can not indicate the stable feature of whole phase space. The stability may vary with different regions in phase space. We have to examine the variability of instability with the evolution of system states to reveal the stable features of whole phase space. As far as predictability is concerned, the range of predictability strongly depends on the initial states. No loss of predictability will occur for the initial states in the basins of equilibrium state attractors in phase space, but predictability will lose at last for the initial states outside the basins. Predictability may also be an initial problem.

The above discussion is concerned with different type of attractor in phase space. In the following, we will focus on the localized features of chaotic attractor itself, and show that predictability may vary with different positions on chaotic attractor.

III. MATHEMATICAL REPRESENTATION OF LOCALIZED FEATURES OF CHAOTIC ATTRACTOR

A few parameters have been proposed to describe the chaotic attractor, such as Lyapunov exponent, Kolmogorov entropy and fractal dimension. These indices can be used well to represent global features instead of localized features. Thus, it is required to develop new notions to give a good description of the localized features of chaotic attractor. One of the basic properties of chaos is its sensitivity to the initial state. In view of such properties, we will introduce finite-time and local-time instabilities to describe localized features.

Consider a real N-dimensional dynamical system with a state vector x, whose evolution equation is

$$\frac{\mathrm{d}x}{\mathrm{d}t} = F(x). \tag{4}$$

The evolution of a small perturbation x' is determined by the linearized counterpart of (1), which can be written as

$$\frac{dx'}{dt} = Ax', \tag{5}$$

where A is the Jacobian of F evaluated at a prescribed time t. Integrating over some portion of trajectory from t_0 to t, we can write Eq. (5) in integral form

$$x(t) = S(t,t_0)x(t_0). \tag{6}$$

Here the "′" has been omitted for the sake of brevity. $x(t_0)$ is a initial perturbation, which can be thought to be error in this study. $S(t, t_0)$ is a linear operator, which is called the resolvent of (5).

We have chosen an inner product such that

$$(x, y) = x^T Dy = y^T Dx. \tag{7}$$

where x and y are N-dimensional vectors. T stands for matrix transpose. D should be a positive symmetrical matrix. The norm of a vector y is $\|y\| = \sqrt{(y, y)}$, and $\|y\|^2$ can be called the generalized energy.

Let

$$\sigma = \frac{\|x'(t)\|}{\|x'(t_0)\|}. \tag{8}$$

σ gives the perturbation growth rate from time t_0 to t. The larger σ is, the more rapidly the perturbations amplify. Obviously, σ is also a measure of sensitivity to the initial state.

From Eq. (6), we can get

$$\|x\|^2 = X(t_0)^T S(t,t_0)^T D S(t,t_0)X(t_0). \tag{9}$$

Let $H = S(t, t_0)^T D S(t, t_0)$, it is easily proved that H is a positive symmetrical matrix. Introduce the generalized eigenvalue problem

$$Hv = \lambda Dv. \tag{10}$$

Because D is a positive symmetrical matrix, we can have decomposition

$$D = LL^T. \tag{11}$$

Substitution of Eq. (11) into Eq. (10) yields

$$(L^{-1}H L^{-T})(L^T v) = \lambda L^T v, \tag{12}$$

where L^{-T} is the transpose of inverse matrix L^{-1}. Let $u = L^T v$. So Eq. (12) becomes the general eigenvalue problem of matrix G with the eigenvector u, where $G = L^{-1}HL^{-T}$. G is also a positive symmetrical matrix. Therefore, all the eigenvectors $u_j (j = 1, 2, 3, \cdots, N)$ of the matrix G will form a complete orthonormal basis in the Euclidean space.

We have

$$v_j = L^{-T} u_j, \tag{13}$$

it can then be obtained

$$(v_i, v_j) = v_i^T D v_j = u_i^T L^{-1} D L^{-T} u_j = u_i^T u_j = \begin{cases} 0, & i \neq j \\ 1, & i = j \end{cases} \tag{14}$$

Thus it has been shown that all v_j's $(j = 1, 2, 3, \cdots, N)$ form a complete orthonormal basis in the given generalized energy inner product space. Let the eigenvalues be such arranged that $\lambda_1 > \lambda_2 > \cdots > \lambda_N$.

A given state vector $x(t_0)$ can be expanded in terms of the eigenvectors:

$$x(t_0) = \sum_{j=1}^{N} \xi_{0j} v_j, \tag{15}$$

where $\xi_{0j} = (x(t_0), v_j)$ is called the projection of the state vector $x(t_0)$ onto the eigenvector v_j. Considering $\|x(t_0)\|^2 = \|\xi_0\|^2$, we substitute Eq. (15) into Eq. (9), then have

$$\|x\|^2 = \xi_0^T \Lambda \xi_0, \tag{16}$$

where $\xi_0 = (\xi_{01}, \xi_{02}, \cdots, \xi_{0N})^T$. Λ is a diagonal matrix, and its diagonal element is λ_j. We can easily get from Eq. (16)

$$\sigma \leqslant \lambda_1, \tag{17}$$

where λ_1 is the generalized eigenvalue associated with v_1. If and only if x_0 is parallel to the eigenvector v_j, Eq. (17) becomes an equality. For such a case, λ_1 is just the growth rate of the perturbation energy error.

We define the finite-time instability for the trajectory portion from time t_0 to t if there exists such an initial perturbation that the generalized perturbation energy will grow. Thus, if $\lambda_1 > 1.0$, the trajectory is unstable. The larger the λ_1 is, the more unstable the trajectory. For the large λ_1, initially close trajectory will disperse rapidly, and the evolution of the system state will be extremely sensitive to the initial state. We also refer to λ_1 as a finite-time instability index.

The above derivation has given the method to calculate λ_1. $S(t, t_0)$ is first evaluated, then the generalized eigenvalue problem is solved. For the dynamical system with small dimension, $S(t, t_0)$ may be evaluated column by column by integrating (5). However, the computation amount will become enormous for the dynamical system with large dimension if the method is still be used. A specific method (Lacarra 1988; Molteni et al. 1993) has now been developed for the case with large dimension.

Now we turn to the discussion of local-time instability. Considering the matrix equation

$$\frac{dS(t, t_0)}{dt} = AS(t, t_0), \tag{18}$$

and referring to Eq. (6), we can obtain

$$\frac{d\|x\|^2}{dt} = x^T(A^T D + DA)x. \tag{19}$$

Let $C = A^T D + DA$. It can be seen that C is a symmetrical matrix. We introduce a generalized eigenvalue problem similar to that for finite-time instability :

$$Cv = \lambda Dv. \tag{20}$$

From the same discussion as above, we can also show that all v_j's ($j = 1, 2, 3, \cdots, N$) form a complete orthonormal basis in the given energy inner product space, and get

$$\frac{d\|x\|^2}{dt} = \xi^T \Lambda \xi, \tag{21}$$

where $\xi_j = (x, v_j)$ is called the projection of the state vector x onto the eigenvector v_j. We can thus have

$$\frac{d\|x\|^2}{dt} = \lambda_j \|x\|^2, \qquad \text{for } x \text{ parallel to } v_j. \tag{22}$$

and

$$\frac{d\|x\|^2}{dt} \leqslant \lambda_1 \|x\|^2. \tag{23}$$

If and only if x_0 is parallel to the eigenvector v_1, (23) becomes an equality. It can be

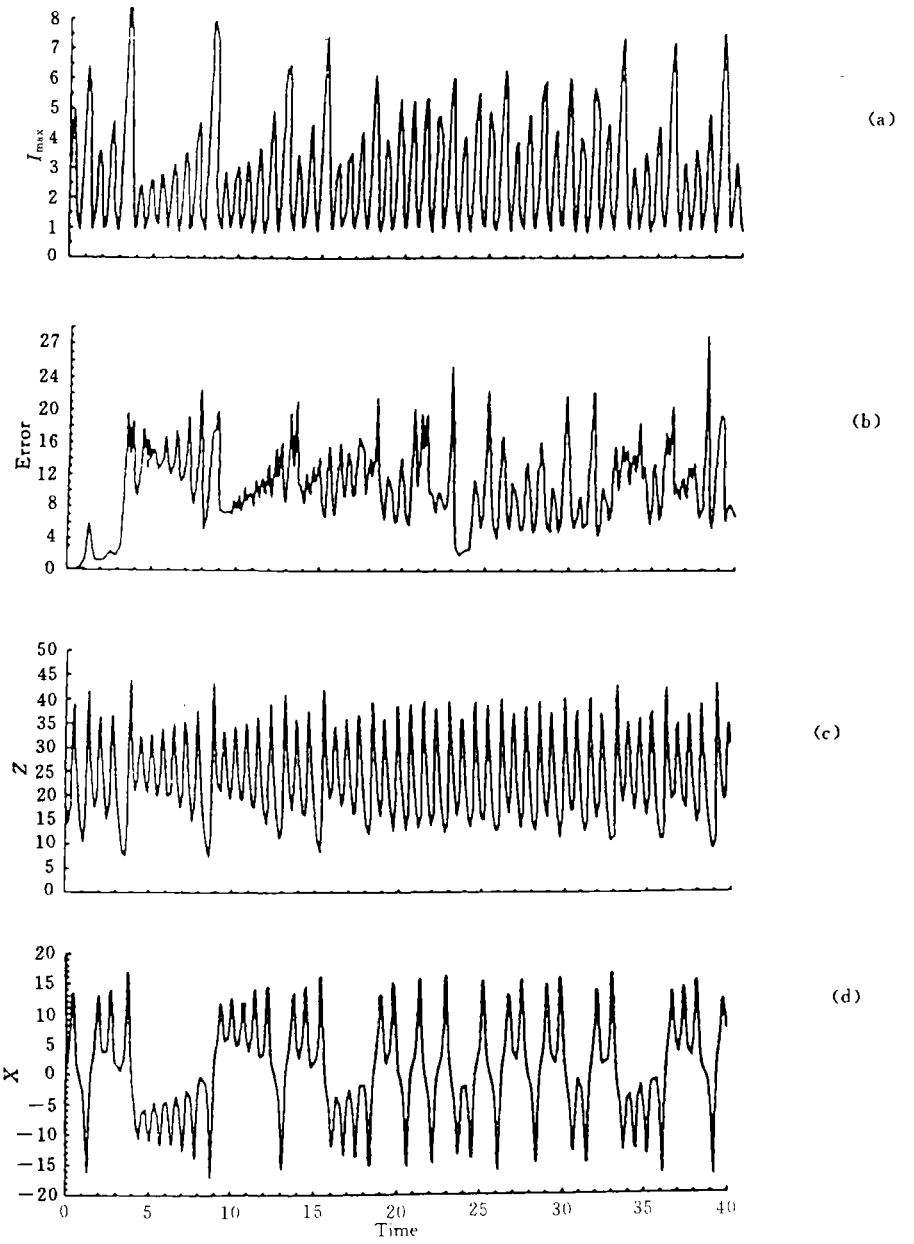

Fig. 3. Evolution of the state of the Lorenz' s system. (a) the index of the finite-time instability for $\triangle t=t-t_0=0.1$: (b) the error evolution from the initial error (0. 2. 0. 2. 0. 2): (c) the evolution of the Z-component: (d) the evolution of the X-component.

found that a perturbation may grow for $\lambda_1>0.0$. Thus we define the trajectory at time t as the local-time instability if $\lambda_1>0.0$. It is noteworthy that the interaction between perturbations selves contributes nothing to the error growth rate for the large-scale atmospheric motion. So Eq. (19) holds independent of the assumption that perturbations have only small amplitude.

From the discussion above, it is obvious that finite-time instability and local-time instability could be power notions to describe the localized features of chaotic system and the variability of its sensitivity to the initial state. In the following, we will show that, as expected, there exist strongly localized features on chaotic attractors.

IV. LOCALIZED FEATURE OF CHAOTIC ATTRACTOR

The famous Lorenz system is used in the following discussion. We take values $\sigma=10$, $b=8/3$ and $\gamma=28.0$. So the system possesses the so-called "standard Lorenz attractor". We will examine the variability of the instability for the trajectory starting from the initial state (1.0, 2.0, 3.0). This initial state is chosen arbitrarily, but different initial values will not change the conclusions. D is taken as an identity matrix here.

1. *For Finite-Time Instability*

We first use the finite-time instability to describe the localized features, and take value $\triangle t=t-t_0=0.1$. Figure 3a shows the evolution of the finite-time instability index λ_1. λ_1 varies considerably with the evolution of the system state. The local maxima have the values about 7.0 to 8.0, i.e. the error can maximally increase to 7 to 8 times as large as that in the initial state during the period of 0.1 time units. But the local minima are close to 1.0 or a little smaller than 1.0, which indicates that the error will not increase and even decrease. Figure 3b presents the time evolution of the root-mean-square error from the small initial error (0.2, 0.2, 0.2). From the comparison between Fig. 3a and Fig. 3b, one can find that the error extremely increases after the instability evolves to a strong maximum. In fact, the error keeps in a small value first, then the error rapidly amplifies to the saturation value during the period of 3 to 4 time units when a strong maximum of instability occurs. For the later evolution, the small perturbation assumption is no longer valid. Nevertheless, it can still be seen that the error maximum seems to correspond to the instability maximum to some extent.

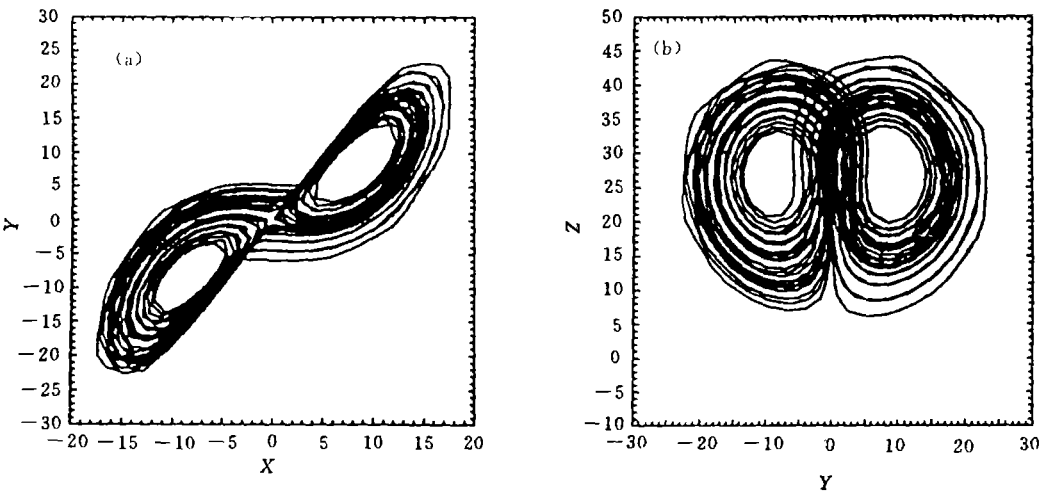

Fig. 4. For $\gamma=28.0$. The trajectory starting from the initial state (1.0, 2.0, 20.0): (a) in the X-Y plane; (b) in the Y-Z plane.

We will show that the chaotic attractor possesses strong localized features. Comparing Fig. 3a with Figs. 3c and 3d, one can see that the maxima of finite-time instability index are well consistent with the minima of the Z-component. This actually indicates that maximum instability may be localized in a fixed region on the attractor. In order to describe the localizability more clearly, we present the distribution of instability indices in phase space. Figure 4a depicts the time evolution of the trajectory on the X-Y plane over the integration time of 40 time units, and Fig. 4b in the Y-Z plane. Figures 5a and 5b show the distribution of the points for $\lambda_1 > 4.0$ corresponding to Figs. 4a and 4b (λ_1 is calculated every 0.05 time units). It can be seen that all strongly unstable points are localized in a small region compared with the attractor itself in both the X-Y plane and the Y-Z plane, which well accord with the position where the ensemble disperses rapidly shown by Palmer (1993). Furthermore, the

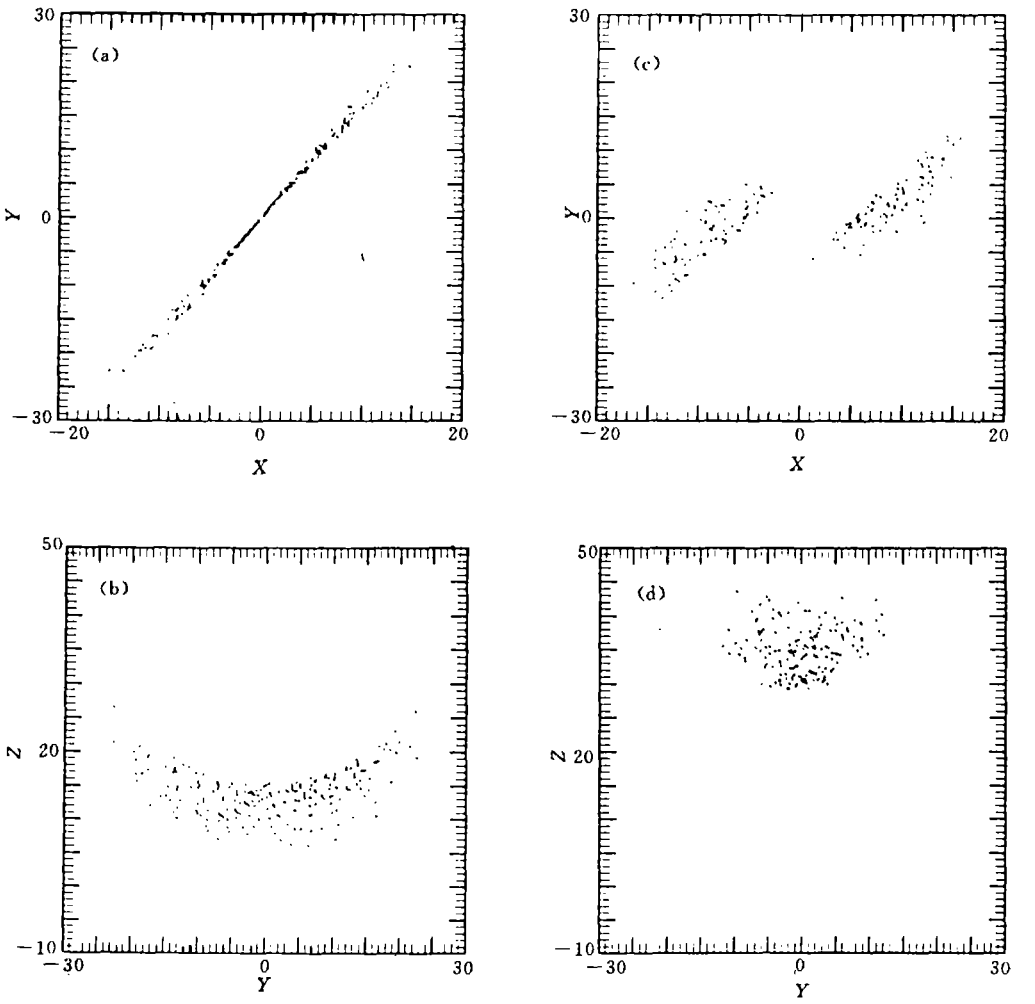

Fig. 5. Corresponding to the trajectory in Fig. 4. The distribution of strong instability in phase space: (a) in the X-Y plane; (b) in the Y-Z plane; (c) and (d) same as in (a) and (b), but for weak instability.

maximum instability is closely related to the evolution feature of the trajectory portion. Comparison of Fig. 3a with Figs. 3c and 3d shows that the maximum instability is associated with the transition of the equilibrium states with which the trajectory circles. However, the transition does not always correspond to strong maximum of the instability. Close examination shows that the transition will accord with the strong maximum of instability only if the Z-component has a small value. In contrast, the instability will be relatively weak for the Z-component with a large value, even though the transition occurs. Therefore, as we have expected, the strong instability is localized in a small region, and associated with the special evolution behavior of the trajectory.

In order to give the localized features of the distribution of weak instability on the chaotic attractors, Figures 5c and 5d present the points for $\lambda_1 < 1.2$. It can be seen that the weak instability is also localized in a very small region. It is of important interest that the region of strong instability is separable from that of weak instability. This further confirms the strong localizability of the chaotic attractor. The localizability strongly suggests that the considerable variation with the position on the chaotic attractors is an essential aspect of predictability, and those indices describing the global property of chaotic attractors may not completely reveal the essence of predictability.

2 . *For Local-Time Instability*

The local-time instability in fact determines the instantaneous error growth rate, and it is independent of small perturbation assumption. The following calculation will further show the strong localizability of the chaotic attractor, and the relationship between finite-time and local-time instabilities will be discussed.

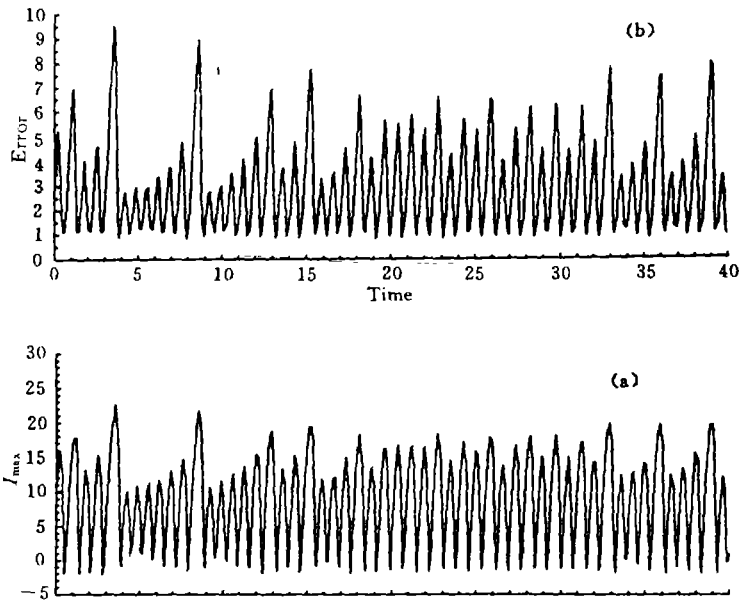

Fig. 6. (a) The evolution of the local-time instability index; (b) the equivalent growth rate for time-interval of 0.1 time units.

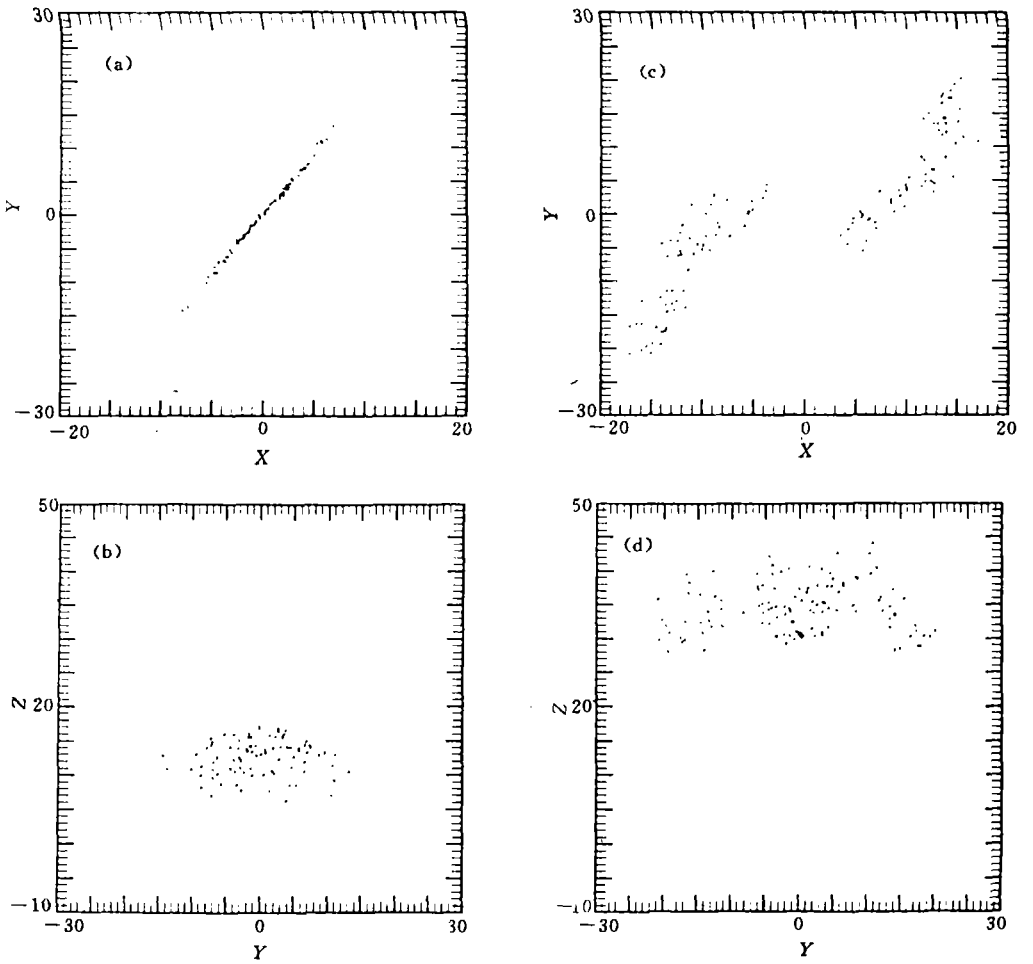

Fig. 7. (a) The distribution of points for equivalent growth rate larger than 4.0 in the X-Y plane; (b) same as in (a), but for the Y-Z plane; (c) and (d), same as in (a) and (b) respectively, but for equivalent growth rate smaller than 1.2.

Figure 6a presents the evolution of the maximum growth rate λ_1. In order to compare it with finite-time instability, we have computed equivalent growth rates for the time interval of 0.1 time units, which is depicted in Fig. 6b. One can see that both the evolution behavior and the magnitude of error growth rate are well consistent with those for finite-time instability. As done for finite-time instability, Figure 7 presents the distribution of points in 2D cuts for the equivalent growth rate larger than 4.0 and smaller than 1.2. Such distribution also accords with that for finite-time instability. Therefore, the analysis of local-time instability further confirms the conclusions obtained above from the calculation of finite-time instability.

V. CONCLUSION AND DISCUSSION

It has been found in the operational numerical weather prediction (NWP) that there is a great deal of case-to-case variabilities of the predictive skill. This fact has attracted extensive interests. The close examination of such phenomenon will benefit us to improve the

understanding of the cause for the loss of predictability and provide us with new line of thought to better use the NWP products as well as to make extended-range forecasts. In the theory of the classic predictability, the parameters describing the global features of chaotic attractor, such as Lyapunov exponent and Reny entropy, are generally used to estimate the range of predictability. But the classic theory can not obviously interpret such variation of predictability. In the present study, we have suggested that the localized features of chaotic attractor have to be studied. Then, we have introduced the notions of finite-time and local-time instability to describe the localized features of chaotic attractor, which determine maximum finite-time and instantaneous error growth rate. These growth rates can be calculated by solving the eigenvalue problems of a positive symmetrical and general symmetrical matrix, respectively.

The famous Lorenz system has been used to exhibit the localized features of chaotic attractor. In the phase space, chaotic and equilibrium state attractors may coexist. For such a case, whether the predictability loses or not completely depends on the initial state. Furthermore, on the chaotic attractor itself, finite-time and local-time instabilities both vary considerably, and the chaotic attractor possesses strong localized features. The strong and weak instabilities are clearly separable from each other in phase space. The loss of predictability results from the error growth only when the system state evolves into strong unstable regions. For an individual prediction, the range of predictability will be large if the system state does not evolve into strong unstable regions. Conversely, the range of predictability will be small. The variation of predictability with the position on the chaotic attractor is its essential aspect. These results suggest that a great deal of case-to-case variabilities of the predictive skill in the operational forecast may be the direct reflection of the localized features of chaotic attractor. Our results also imply that the variability of the predictive skill may exist even for the complete NWP model. It is noteworthy that the analysis of the operational products has been indicative of the relationship between the variability of the predictive skill and the localized features of the chaotic atmospheric attractor in the phase space, which will be presented in another paper.

We are grateful to Prof. Chou Jifan for his useful comments on the earlier version of the manuscript. This research was supported in part by the state key laboratory LASG.

REFERENCES

Branstator, G. (1986). The variability in skill of 72-hour global scale NMC forecasts, *Mon. Wea. Rea.*, **114**: 1384—1392.

Charney, J. G. et al. (1966). The feasibility of a global observation and analysis experiment, *Bull. Amer. Meteor. Soc.*, **47**: 200—220.

Chou Jifan. (1990). *The New Advance in Atmospheric Dynamics*. Lanzhou University Press, pp. 22—28 (in Chinese).

Fraedrich, K. (1987). Estimating the weather and climate predictability on attractor, *J. Atmos. Sci.*, **44**: 1384—1392.

Hollingworth, A. et al. (1987). Mid-latitude atmosphere prediction on time scale of 30 days, *Variability in the Atmosphere and Oceans*, Ed. H. Cattle. Roy. Meteorol. Soc.

Lacarra, J-F. et al. (1988). Short-range evolution of small perturbation in a barotropic model, *Tellus*, **40**A: 81—95.

Leith, C. E. (1965) Numerical simulation of the earth' s atmosphere. *Method in Computional Physics*, 4. New York, Academic Press.

Li Zhijin and Ji Liren (1994). The instability of trajectory and error growth. *Acta. Meteor. Sin.*, **8**: 392—402.

Lorenz, E. N. (1963). Deterministic nonperiodic flow. *J. Atmos. Sci.*, **23**: 130—141.

Lorenz, E. N. (1969). Atmospheric predictability as revealed by naturally occurring analogues. *J. Atmos. Sci.*, **26**: 636—646.

Lorenz, E. N. (1984). Irregularity: fundamental property of the atmosphere. *Tellus*, 36A, **2**: 98—110.

Molteni, F. et al. (1993). Predictability and finite-time instability of the northern winter circulation. *Quart. J. Meteor. Roy. Soc.*, **119**: 269—298.

Mukougawa, H. et al., (1991). A relationship between local error growth and quasi-stationary states in the Lorenz system. *J. Atmos. Sci.*, **48**: 1231—1237.

Palmer, T. N. (1993). Extended-range atmospheric prediction and the Lorenz model. *Bulltin Amer. Meteor. Soc.*, **74**: 49—65.

Smagrinsky, J. (1963). General circulation experiments with the primitive equations. I: The basic experiment. *Mon. Wea. Rev.*, **91**: 99—164.

Wolf, A. et al. (1985). Determining Lyapunov exponents from a time series. *Physica*. **16**d: 285—317.